PAPER

Development of highly selective and sensitive molecularly imprinted polymer-based electrochemical sensors for tolvaptan assay in tablet and serum

Received 00th January 20xx,
Accepted 00th January 20xx

DOI: 10.1039/x0xx00000x

Leyla Karadurmus,*[a] Fatma Budak, [bc] Ahmet Cetinkaya, [bc] Esen Bellur Atici [d] and Sibel A. Ozkan *[b]

In this research, two different molecularly imprinted polymer (MIP)-based electrochemical sensors were proposed for the determination of tolvaptan (TOL). Photopolymerization (PP) and thermal polymerization (TP) techniques were developed for the determination of TOL. The advantages of MIP were used to design an electrochemical sensor for selective and sensitive determination of TOL. TOL was determined on glassy carbon electrode (GCE) using differential pulse voltammetry (DPV) for both techniques. Some important parameters affecting the sensor efficiency, such as template/monomer ratio, PP and TP time, drop volume, removal solutions, removal and rebinding time, etc., were optimized. The surface characterization of the proposed MIP-based electrochemical sensors was carried out with electrochemical characterization by electrochemical impedance spectroscopy (EIS) and cyclic voltammetry (CV) methods. It was extended with scanning electron microscopy (SEM) technique. Under optimal conditions, the developed sensors showed good linearity between 1.0 × 10^{-11} M to 1.0 × 10^{-10} M and 2.5 × 10^{-11} M to 2.5 × 10^{-10} M for PP and TP, respectively. Low detection limits (2.89 × 10^{-12} M (PP) and 1.88 × 10^{-13} M (TP)) were also obtained for TOL determination. The applicability of the proposed sensor was evaluated using tablet and commercial human serum samples. Interference and imprinting factor studies verified the selectivity and specificity of the proposed sensors, and the efficiency of the sensors was verified using unprinted polymer for comparison at each step.

1. Introduction

Arginine vasopressin and renin-angiotensin-aldosterone are receptors which have the role of regulating body fluids. Tolvaptan, *i.e.* (TOL, *N*-(4-(7-chloro-5-hydroxy-2,3,4,5-tetrahydro-1*H*-benzo[*b*]azepine-1-carbonyl)-3-methylphenyl)-2-methylbenzamide), is a new class drug, a “vaptan", that antagonizes with the neurohormone arginine vasopressin receptors. In clinical evaluation, it has been shown to be effective in the treatment of hyponatremia and may have a more beneficial effect than current treatments. Although traditional diuretics have been used to treat heart failure, they can damage renal function. TOL, as a recently proposed vasopressin-2 receptor antagonist, induces aquaresis and improves volume overload in heart failure.[1–3]

The analysis of TOL by spectroscopic, [4–6] chromatographic,[7,8,17,18,9–16] and electrochemical techniques[19] has been reported. The methods for determination of TOL have been discussed in terms of sample handling, cost, and sensitivity. The method for detecting TOL in pharmaceutical dosage forms and biological fluids needs to be improved due to the difficulties encountered.

Many researchers have considered the use of electrochemical methods for the determination of pharmaceutical compounds due to their advantages such as affordability, high level of sensitivity, easiness of use, low assay time and sensing capabilities. One electrochemical technique has been used to detect TOL in biological samples and pharmaceutical dosage forms, including multi-walled carbon nanotube (MWCNT) modified carbon paste electrode using differential pulse voltammetry [19]. Various analytical parameters, scan rate, accumulation time, accumulation potential, and pH, have been optimized to develop a simple and economical method for determining TOL. The limit of detection (LOD) and limit of quantification (LOQ) were found to be 3.81 x 10^{-8} M and 1.27 x 10^{-7} M, respectively. The method successfully detected TOL in pharmaceutical preparations and biological samples. The challenges associated with improving the analytical properties of sensors, which include sensitivity, selectivity and analytical application stability, are the main reasons why researchers are seeking new ways to modify and improve the electrochemical sensors. In fact, sensor selectivity is one of the most critical parameters since the sensors must respond to analytes in complex matrixes.

[a] Adıyaman University, Department of Analytical Chemistry, Faculty of Pharmacy, Adıyaman, Türkiye.
[b] Ankara University, Faculty of Pharmacy, Department of Analytical Chemistry, 06560, Ankara, Türkiye.
[c] Ankara University, Graduate School of Health Sciences, Ankara, Türkiye
[d] DEVA Holding A.Ş., R&D Center, 59510 Kapaklı, Tekirdağ, Türkiye.
*leylakrdrms@gmail.com, Sibel.Ozkan@pharmacy.ankara.edu.tr
Electronic Supplementary Information (ESI) available: [Information on reagents and chemicals, equipment, preparation of commercial human serum samples and pharmaceutical dosage form, and surface characterization is provided in the Supplementary Materials file]. See DOI: 10.1039/x0xx00000x

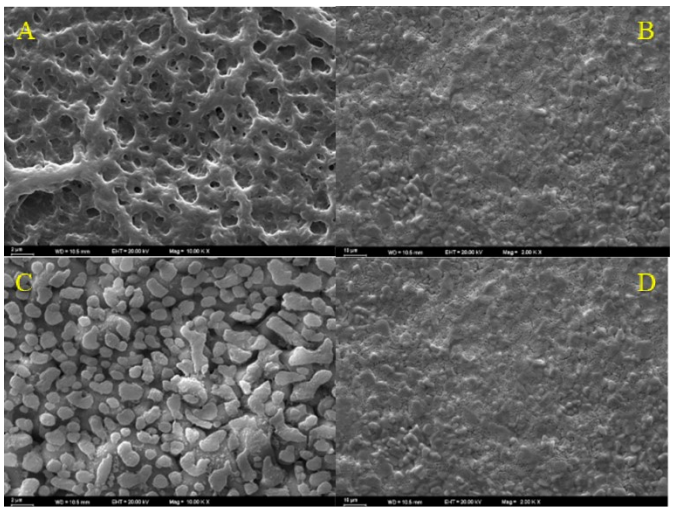

Fig. 1 The characterization of the electrode surface. SEM images of PP A) MIP and B) NIP surfaces and TP C) MIP and D) NIP.

The development of molecularly imprinted polymer (MIP)-based electrochemical sensors is rapidly emerging as a new technology for performing selective and sensitive assays of target compounds in various fields such as drug testing, food analysis, environmental monitoring, and clinical diagnostics [20,21]. MIPs can selectively detect a template molecule easily and quickly [22,23]. The synthesis procedure is simple and inexpensive, and MIPs are stable under harsh conditions. MIPs are designed by polymerizing a cross-linking agent and an appropriate monomer in the presence of the target compound. After polymerization, the template is removed from the polymeric matrix, leaving voids that complement the shape and size of the target so that the analyte can be specifically bound [24,25].

So far, electrochemical nanosensors study has been performed to determine TOL. For the first time, MIP-based electrochemical sensors have been synthesized for TOL. By combining the advantages of MIP technique and electrochemical method, the aim of this work is to develop a MIP-based electrochemical sensor with excellent selectivity and high sensitivity against TOL drug. The developed MIP-based electrochemical sensor was fabricated on the GCE surface as a thin film layer. TOL showed high sensitivity and selectivity to the template molecule in the designed sensor. The developed sensor used 4-aminophenol (4-AP) as the monomer, ethylene glycol dimethacrylate (EGDMA) as the crosslinking agent for the MIP synthesis, and a MIP-based electrochemical sensor was designed on the GCE surface by the thermal polymerization method. In the designed sensor, TOL showed very high sensitivity and selectivity towards the template molecule. Electrochemical impedance spectroscopy (EIS), cyclic voltammetry (CV) and scanning electron microscopy (SEM) were used to characterize the MIP-based electrochemical sensor. For the quantitative determination of TOL, 5.0 mM $[Fe(CN)_6]^{3-/4-}$ were measured with a redox probe in solution using the differential pulse voltammetry (DPV) technique. Furthermore, the proposed sensor was successfully applied to detect TOL in tablets and commercial human serum samples.

2. Experimental

Information on reagents and chemicals, equipment, preparation of commercial human serum samples and pharmaceutical dosage form, and surface characterization is provided in the Supplementary Materials file.

2.1. Preparation of MIP/GCE sensor

Prior to each experiment, the electrode was sonicated in ethanol and ultrapure water (1:1) for 10 min. The GCE was then polished by dripping alumina onto the polishing pad and rinsed with ultrapure water. It was dried at room temperature.

One of the MIPs was developed on GCE by copolymerization of 4-AP and hydroxyethyl methacrylate (HEMA) with cross-linking ethylene glycol dimethacrylate (EGDMA) in the presence of TOL. Under optimum conditions, the developed sensor was fabricated by keeping it under a UV lamp at room temperature. Acrylic acid (AA) was used as monomer to prepare thermal polymerization MIP/GCE. 10 µL of sodium dodecyl sulfate (SDS) and 10 µL of ammonia solution (NH_3) were used to create the porous structure in the prepared mixed solution. After sonicating the mixed solution, 10 µL of TEOS were added to the solution. Finally, 1.75 µL of solution were dropped on the electrode surface and dried in the oven at 60 °C for 20 min.

Experimental parameters such as template/monomer ratio, removal solutions, drop volume, polymerization time, removal and rebinding time were investigated for both MIP-based sensors. Imprinting factors (IFs) were calculated using substances with similar chemical structures to test the selectivity of the sensor. The experimental results indicated that the proposed sensor for TOL was selective and sensitive in commercial human serum and tablet samples. The control measurements were performed using non-imprinted polymer (NIP) prepared without the addition of TOL using the same procedure performed for MIPs.

3. Results and discussion

3.1. Surface characterization of MIP/GCE

Scanning electron microscopy (SEM) measurements were used to perform a detailed morphological analysis of the sensor surface based on molecularly imprinted polymers (MIPs) and to compare it with the surface based on non-imprinted polymers (NIPs) (Figure 1). Our purpose was to evaluate the structural characteristics of both surfaces and to identify any notable differences. For the 4-AP-TOL-MIP(PP)/GCE and AA-TOL-MIP(TP)/GCE sensors, the SEM images revealed distinct differences between the MIP and NIP surfaces. As expected, the MIP surface exhibited a rough and porous texture indicative of the imprinting process. This roughness and porosity are the result of the specific binding sites created by the MIPs, which are designed to selectively capture the target analyte (Figure 1A and Figure 1C). In contrast, SEM analysis of the NIP-based surface (Figure 1B and Figure 1D) showed a smooth texture with minimal irregularities. This lack of roughness and porosity is expected since NIPs do not possess the selective binding sites characteristic of MIPs. These results confirm that the MIP-based sensor surface has the desired morphological characteristics, while the NIP-based surface serves as a suitable control.

3.2. Electrochemical characterization of MIP/GCE sensor

The electrochemical characterization of MIP/GCE and MIP/GCE sensors was also evaluated using CV and EIS methods. These methods are fundamental techniques that describe the conductivity of the electrode surface, the change transfer resistance, and the electron transfer process. The electrochemical behavior of the MIP/GCE and MIP/GCE sensors was performed using a 5 mM $[Fe(CN)_6]^{3-/4-}$ solution as a redox probe. The sensors were characterized by evaluating the peak current and resistance values obtained during the preparation stages such as bare GCE, after polymerization, after removal, and after rebinding. The CV and EIS plots for each step of the PP and TP processes are shown in Figure 2. In both processes (Figure 2A and Figure 2C), the peak current values of $[Fe(CN)_6]^{3-/4-}$ peak current were obtained as the maximum because there are no factors preventing electron transfer on the bare GCE surface (black line). After the polymerization processes, the peak intensity of the $[Fe(CN)_6]^{3-/4-}$ peak current was lost because the GCE surface was covered by a polymer film that prevented electron transfer (red line). After removing the TOL molecule from the polymer film, specific cavities for TOL formed and the $[Fe(CN)_6]^{3-/4-}$ peak current observed turned out to be lower than the one from the bare GCE (blue line). Finally, the peak values obtained by rebinding the known concentration of TOL were lower than those obtained after removal due to the closure of the cavities on the polymer film (green line). In the EIS measurements, Nyquist plots and changes in charge transfer resistance (R_{ct}) were evaluated (Figure 2B, Figure 2D) and the same steps were applied. According to the EIS results, the bare GCE surface has the lowest R_{ct} values (black dots) because electron transfer is easily realized. Since the formation of polymer films on the GCE surface after polymerization prevents electron transfer, the R_{ct} values (red dots) reach the highest value. After removal of the TOL molecules, specific voids are formed on the GCE surface. When the TOL molecules are removed, specific gaps are formed on the MIP surfaces and the R_{ct} values (blue dots) decrease with the realization of electron transfer. However, upon rebinding of the TOL, the gaps are partially filled, making electron transfer difficult and causing the R_{ct} values (green dots) to increase again. This confirms that TOL molecules selectively bind to specific cavities in the developed MIP sensors.

3.3. Optimization of MIP fabrication

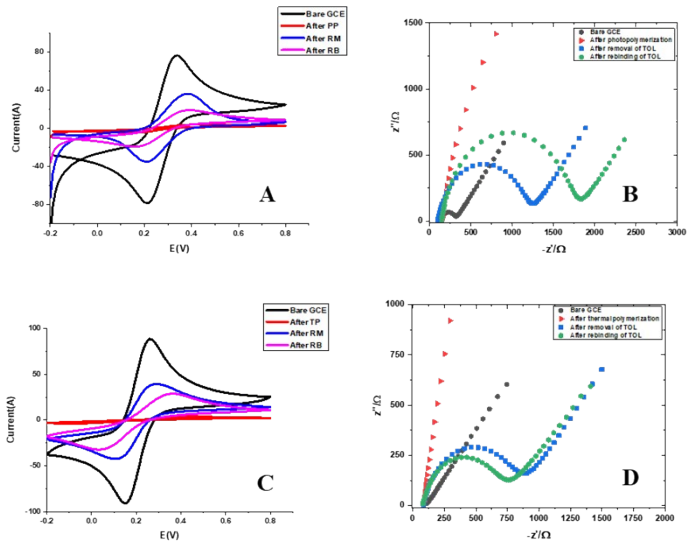

Fig. 2 (A) CV, and (B) EIS measurements of bare GCE, after PP, after removal, and after rebinding of TOL; (C) CV, and (D) EIS measurements of bare GCE, after TP, after removal, and after rebinding of TOL in 5 mM $[Fe(CN)_6]^{3-/4-}$ solution (0.1 M KCl).

Table 1 Results of optimizing parameters affecting sensor response.

Parameters	PP		TP	
	Range	Selected value	Range	Selected value
Template / Monomer ratio	1:1 – 1:5	1:2	1:1 – 1:5	1:2
Dropping volume(µL)	0.25 – 1.25	0.50	1.00 – 2.00	1.75
Polymerization time (min)	3 – 15	5	10 – 40	30
Removal time (min)	3 – 20	10	5 – 25	10
Rebinding time (min)	3 – 15	3	5 – 25	10

The evaluation and optimization of the molecular printed film is the most critical phase of MIP-based sensor fabrication. The results of some optimization parameters affecting the sensor response are shown in Table 1.

Template/monomer ratio. Optimization of the template/monomer ratio is critical to producing efficient and stable polymer films. Since the formation of polymer films is directly related to the interactions between the template and the monomer, the optimal ratio should be determined. In molecular imprinting techniques, the template/monomer ratio can also improve sensor selectivity. However, using too much monomer can lead to a non-selective electrochemical reaction for the template, which can also lead to the deformation of the imprinting sites. Therefore, different monomer/template ratios (1:1, 2:1, 3:1, 4:1, and 5:1) were used for polymer films prepared with PP and TP, and the differences between the peak currents obtained after removal and after polymerization were calculated (Figure S2A and Figure S3A). According to the ΔI values obtained with both PP and TP, the optimal ratio was selected as 1:2 for both sensors, which provided the most stable and efficient polymer.

Dropping volume. The drop volume on the GCE surface is directly related to the thickness of the polymer film and the polymer formation process and needs to be optimized. Therefore, different drop volumes (0.25 – 1.25 µL for PP and 1.00 – 2.00 µL for TP) were dropped on the GCE surface and optimized for the developed MIP/GCE sensors to obtain a good polymer film in terms of conductivity, diffusion limitation, and thickness. It was evaluated by taking the difference between the peak currents obtained after removal and after polymerization, being the optimal drop amount volumes obtained as 0.50 µL and 1.75 µL for PP and TP, respectively (Figure S2B and Figure S3B).

Polymerization time. The 4-AP-TOL-MIP(PP)/GCE sensor was prepared under a UV lamp with a wavelength of 365 nm and a power density of 100 W. By optimization of the PP time under the UV lamp, a stable polymer film was formed on the GCE surface. After dropping 0.50 µL of polymerization solution on the GCE surface, it was exposed to UV light for 3 – 15 min. The differences in the peak currents after removal and after PP were then compared. Considering that the sensor preparation time is not very long, being a polymerization time of 5 min chosen as the most optimal (Figure S2C).

Thermal polymerization was performed in an oven (50 °C) for 30 min. Then, 1.75 µL of polymerization solution was dropped on the GCE surface, and it was exposed to the oven for 10 – 40 min. The differences in the peak currents after removal and after TP were then compared. Considering that the preparation time of the AA-TOL-MIP(TP)/GCE sensor is not very long, 30 min was chosen as the optimal polymerization time (Figure S3C).

Removal solution and time. Removing template molecules from MIP films without damaging the polymer film is a critical step. In this part, specific cavities are formed after the template molecule is removed and the analyte can easily attach to these cavities. Therefore, suitable stripping solutions were selected for both PP and TP. For PP, different removal solutions such as acetone, methanol (MeOH), 10.0 M acetic acid (HAc), 5.0 M sodium hydroxide (NaOH) and 1.0 M hydrochloric acid (HCl) were tested. The method was evaluated by taking the difference between the peak currents of the solvents after removal and after PP. When the effects on the removal process were examined, the peak currents obtained using HAc (10.0 M) were higher than those of other solvents and were selected as the removal solvent (Figure S2D). In the removal process, the modified sensor immersed in 10.0 M HAc was incubated for different times (3 – 20 min) using a ThermoShaker (600 rpm, 25 ºC). The removal time was evaluated by taking the difference between the peak currents after removal and after PP. The best removal time for PP was found to be 10 min (Figure S2E).

Table 2 Validation of the MIP-based sensors used for the determination of TOL.

	Standard solution		Serum sample	
	PP	TP	PP	TP
Linearity range (M)	1.0×10^{-11} – 8.0×10^{-11}	2.5×10^{-11} – 2.5×10^{-10}	1.0×10^{-11} – 8.0×10^{-11}	2.5×10^{-11} – 2.5×10^{-10}
Slope (μA/M)	9.44×10^{11}	4.01×10^{11}	7.86×10^{11}	8.30×10^{11}
Intercept (μA)	58.62	75.98	78.75	-1.84
Correlation coefficient	0.998	0.997	0.995	0.999
LOD (M)	2.89×10^{-12}	1.88×10^{-13}	5.97×10^{-13}	2.09×10^{-12}
LOQ (M)	9.62×10^{-12}	6.27×10^{-13}	1.99×10^{-12}	6.95×10^{-12}
Repeatability of peak current (RSD %)*	0.85	0.33	0.96	0.84
Reproducibility of peak current (RSD %)*	1.06	0.59	1.14	1.76

**Each value is average of five measurements.*

For TP, the removal solutions including HAc (15.0 M), ethanol (EtOH), NaOH (1.0 M), HCl (5.0 M), acetone, and acetonitrile (ACN) were tested, and 15.0 M HAc was determined as the best removal solution according to its proper removal efficiency (Figure S3D). In the removal process, the modified sensor immersed in 15.0 M HAc was incubated for different periods of time (5 - 25 min) using a ThermoShaker (600 rpm, 25 ºC). The removal time was evaluated by taking the difference between the peak currents after removal and after TP. The best removal time for TP was found to be 10 min (Figure S3E).

Rebinding time. The rebinding procedure is an important parameter that determines the analysis time and performance. Therefore, the MIP-based sensor prepared for PP was immersed in an 8×10^{-11} M TOL solution to evaluate its effect on rebinding at different times (3 – 15 min) and examined using a ThermoShaker (600 rpm, 25 ºC). When the difference between the peak currents after rebinding and after detachment was evaluated, it was seen that ΔI remained almost the same after reaching the highest value at 10 min. Therefore, according to Figure S2F, the rebinding time was selected as 3 min for the 4-AP-TOL-MIP(PP)/GCE sensor.

The same steps as for PP were performed for TP. The MIP-based sensor prepared for TP was immersed in 2.5×10^{-11} M TOL solution to evaluate its effect on rebinding at different times (5 – 25 min) and performed using ThermoShaker (600 rpm, 25 ºC). By calculating the difference between the peak currents after rebinding and after removal, the optimal rebinding time for stable and efficient binding was found. According to Figure S3F, the rebinding time for the AA-TOL-MIP(TP)/GCE sensor was selected as 10 min.

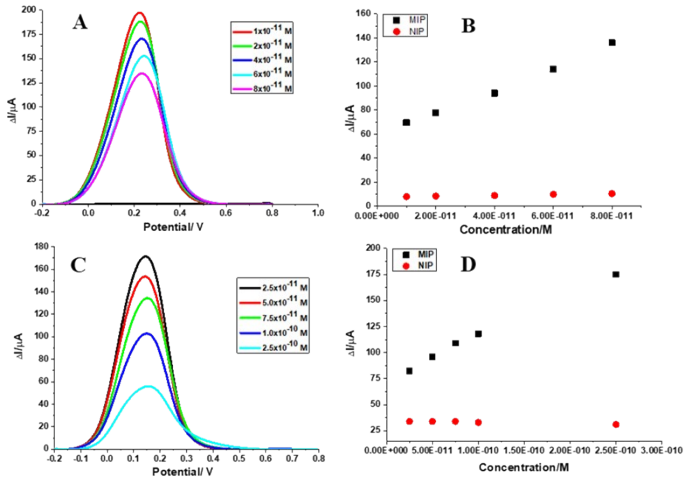

Fig. 3 DPV of TOL on MIP/GCE (A) A linear relationship between the ΔI and TOL concentrations in MIP/GCE and NIP/GCE (B) for PP, (C) A linear relationship between the ΔI and TOL concentrations in MIP/GCE and NIP/GCE (D) for TP.

3.4. Analytical validation of MIP/GCE sensors

The analytical performance of 4-AP-TOL-MIP(PP)/GCE and AA-TOL-MIP(TP)/GCE sensors was evaluated using different concentrations of TOL in a standard solution under optimal conditions. The linearity range of TOL for 4-AP-TOL-MIP(PP)/GCE was obtained using the DPV technique in 5.0 mM $[Fe(CN)_6]^{3-/4-}$ solution as 1.0×10^{-11} – 8.0×10^{-11} M. DP voltammograms and linear curves of this sensor are shown in Figure 3A and Figure 3B, respectively. A linear curve was obtained using ΔI values versus different TOL concentrations. The calibration equation of the 4-AP-TOL-MIP(PP)/GCE sensor was obtained as $\Delta I(\mu A) = 9.44\times10^{11}\,(\mu A/M)\times C(M) + 58.62\,(\mu A)$ (r = 0.998) (Table 2). The LOD and LOQ values were calculated using the formulas 3 × s/m and 10 × s/m (s: standard deviation, m: slope) 20,21 and were found to be 2.89×10^{-12} and 9.62×10^{-12} M, respectively.

The determination of TOL in the concentration range of 2.5×10^{-11} and 2.5×10^{-10} M was performed using both MIP and NIP-based sensors (Figure 3C). The DP voltammograms obtained for TOL on the AA-TOL-MIP(TP)/GCE sensor are shown in Figure 3D. The regression equation was calculated to determine the linearity of the sensor developed for the determination of TOL. Also, using the data of the linear curve obtained by plotting the ΔI values against the TOL concentration, the calibration equation of the AA-TOL-MIP(TP)/GCE sensor was found as $\Delta I(\mu A) = 4.012\times10^{10}\,(\mu A/M)\times C\,(M) + 75.98\,(\mu A)$ (r = 0.997). According to the obtained LOD (1.88×10^{-13} M) and LOQ (6.27×10^{-13} M) values, the sensor developed for the determination of TOL showed very high sensitivity and selectivity. The analytical performances of both 4-AP-TOL-MIP(PP)/GCE and AA-TOL-MIP(TP)/GCE sensors were tested with NIP sensors prepared in the absence of TOL. The results showed that the developed sensors have excellent selectivity and sensitivity for the detection of TOL.

3.5. Application of MIP/GCE sensor to commercial human serum and tablet dosage forms

The developed sensors were used to determine TOL in tablet and commercial human serum samples according to the experimental procedure. These results indicate that the developed sensor is suitable for the analysis of TOL in tablet and serum samples. The responses of the 4-AP-TOL-MIP(PP)/GCE and AA-TOL-MIP(TP)/GCE sensors were linear in different TOL concentration ranges in commercial human serum samples (Table 2), and the linear regression equations of the developed sensors are given below:

$$\Delta I(\mu A) = 7.86\times10^{11}\ (\mu A/M) \times C\ (M) + 78.749\ (\mu A)\ (r = 0.995)$$

(for 4-AP-TOL-MIP(PP)/GCE)

$$\Delta I(\mu A) = 8.304\times10^{11}\ (\mu A/M) \times C\ (M) - 1.840\ (\mu A)\ (r = 0.999)$$

(for AA-TOL-MIP(TP)/GCE)

DPV voltammograms obtained using 4-AP-TOL-MIP(PP)/GCE and AA-TOL-MIP(TP)/GCE as standards are shown in Figure 4A and Figure 4C. The NIP-based sensors were also used to validate the applicability of the MIP-based sensors, and the nonlinearity of the NIP-based sensors versus the MIP-based sensors was observed (Figure 4B and Figure 4D). The excellent recovery and %RSD results in tablet and commercial human serum samples with satisfactory accuracy and applicability were obtained with the 4-AP-TOL-MIP(PP)/GCE and AA-TOL-MIP(TP)/GCE sensors (Table 2). In addition, the performance of the methods used was evaluated by comparing the results obtained using Student's t-test and Fisher's tests. The comparison is presented in Table 3. It was observed that the values obtained by the methods were lower than the theoretical values, indicating that there was no significant difference.

Table 3 Recovery studies for commercial human serum and tablet dosage form samples

	Tablet dosage form		Serum sample	
	PP	TP	PP	TP
Label amount (mg)	30.00	30.00	–	–
Found amount (mg)*	30.40	30.20	–	–
RSD%	0.62	0.75	–	–
Bias%	−1.33	−0.67	–	–
Calculated t_{value}	0.127		–	–
Calculated F_{value}	0.019		–	–
Spiked amount (mg)	5.00	5.00	5.00	5.00
Found amount (mg)*	5.07	5.05	4.96	4.93
Average recovery (%)	101.40	101.00	99.20	98.60
RSD%	0.88	1.23	1.12	1.01
Bias%	−1.40	−1.00	0.80	1.40

Each value is the mean of five experiments. Theoretical student-t and F values are 2.13 and 6.26, respectively.

3.6. Specificity studies via imprinting factor

The most important feature of MIP-based sensors is that they have specific recognition sites with high affinity for the target molecule. In order to demonstrate this feature, similarly structured molecules (tolvaptan metabolite Tol-Ox, regorafenib, sorafenib, nilotinib, imatinib, and dasatinib) were screened, and ΔI_2 values for MIP and NIP corresponding to these molecules were found by the DPV obtained in 6×10^{-11} M concentration for each molecule. The imprinting factor (k) was calculated by the ratio of this value obtained for each molecule to the value obtained for TOL. The ratio of the k values obtained for MIP and NIP to each other represents the relative k (k') value. The k' values higher than 1 point to a high specificity for the target molecule. Structures of the drug substances and the results demonstrating the specificity of 4-AP-TOL-MIP(PP)/GCE and AA-TOL-MIP(TP)/GCE sensors are presented in Table 4. Especially considering the similarity of the structures of tolvaptan (TOL) and its metabolite Tol-Ox which forms via oxidation of the hydroxyl group to a ketone, the specificity of the developed sensor is remarkable.

3.7. Selectivity studies via interference effect

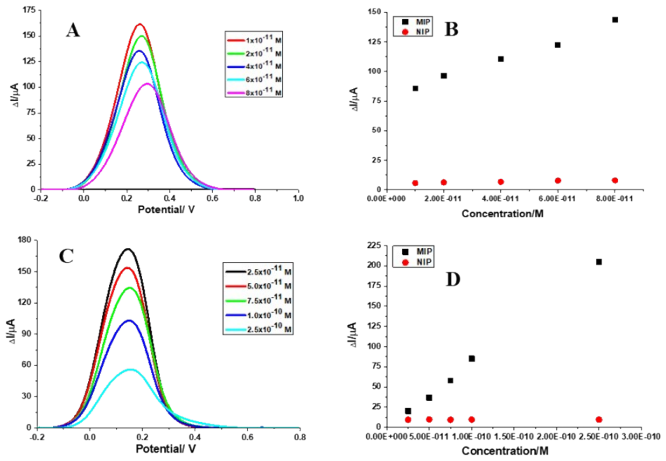

Fig. 4 In spiked serum samples, DPV of TOL on MIP/GCE (A) A linear relationship between the ΔI and TOL concentrations in MIP/GCE and NIP/GCE (B) for PP, (C) A linear relationship between the ΔI and TOL concentrations in MIP/GCE and NIP/GCE (D) for TP.

Table 4 Specificity of the developed MIP-sensors for the determination of TOL.

Molecules	PP			TP		
	MIP (k)	NIP (k)	(k')	MIP (k)	NIP (k)	(k')
Tolvaptan (TOL)	114	27	–	109	34	–
Tol-Ox	4.07	1.37	2.97	5.31	1.70	3.13
Regorafenib	7.12	2.24	3.17	2.95	0.96	3.05
Sorafenib	4.56	1.27	3.61	2.17	0.69	3.12
Nilotinib	4.73	1.41	3.35	4.97	1.59	3.12
Imatinib	3.93	1.11	3.53	7.18	2.24	3.21
Dasatinib	5.43	1.34	4.05	3.45	1.10	3.13

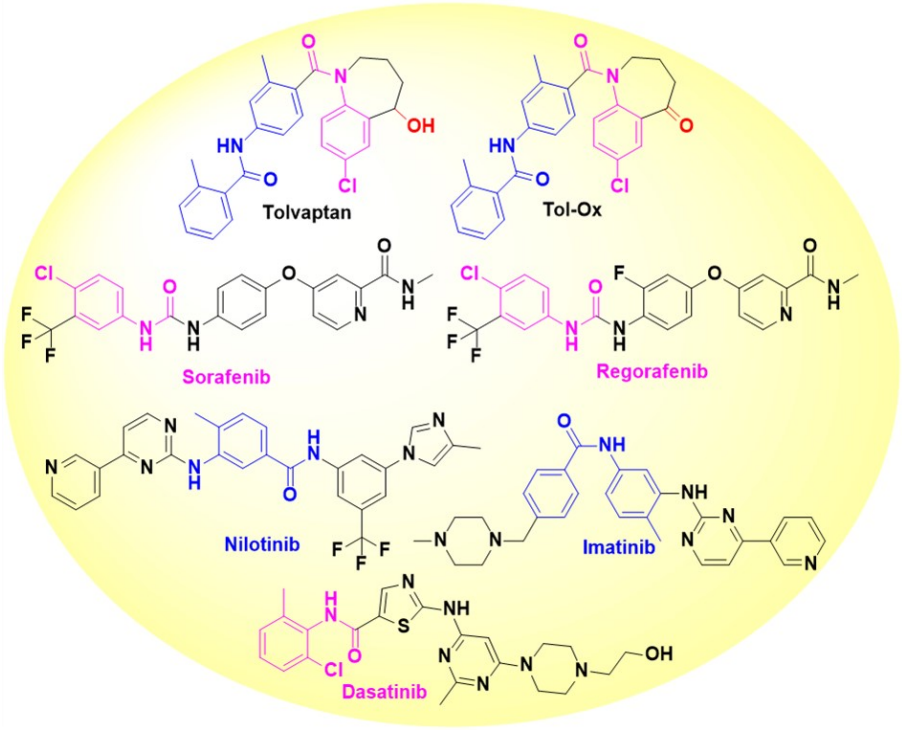

Tests performed with MIP-based sensors may be interfered by compounds naturally present in biological fluids or excreted because of drugs taken by the individual. The 4-AP-TOL-MIP(PP)/GCE and AA-TOL-MIP(TP)/GCE sensors were tested for selectivity at 4.0×10^{-11} M and 2.5×10^{-11} M TOL concentrations, respectively. It was found that the potential interfering agents (IA), that include dopamine, ascorbic acid, uric acid, paracetamol, K^+, NO_3^-, Na^+, SO_4^{2-}, Mg^{2+} and Cl^-, did not affect the response of the developed sensors when they were present at 10 times the concentration of TOL in a solution. The recovery % results of TOL in the presence of interfering agents varied between 98.96 % and 102.83 % (Table S1). RSD values for 4-AP-TOL-MIP(PP)/GCE and AA-TOL-MIP(TP)/GCE sensors were ≤ 1.85 % and ≤ 1.97 %, respectively.

3.8. Stability

Storage stability experiments demonstrated the applicability and reusability of the proposed sensors. As a result of the experiments, it was found that effective results can be obtained in up to seven days with PP, and this period remains within three days with TP. According to this information, it can be said that the sensor developed with PP for TOL has higher stability.

Conclusions

In this study, two different MIP-based electrochemical sensors were developed for the sensitive and selective detection of TOL at very low concentrations. The proposed sensor has simplicity, good stability, good reproducibility, and low cost. The 4-AP-TOL-MIP(PP)/GCE sensor was developed with 4-AP monomer via PP, while the AA-TOL-MIP(TP)/GCE sensor was prepared via TP with AA monomer. Considering the optimization parameters of the 4-AP-TOL-MIP(PP)/GCE sensor, the preparation time was shorter than that of the AA-TOL-MIP(TP)/GCE sensor. However, the AA-TOL-MIP(TP)/GCE sensor outperformed the 4-AP-TOL-MIP(PP)/GCE sensor in terms of LOD and LOQ values. Morphological (SEM) and electrochemical (CV and EIS) characterizations of the 4-AP-TOL-MIP(PP)/GCE and AA-TOL-MIP(TP)/GCE sensors were performed, and the results were discussed in detail. Stability studies were performed to demonstrate the reusability and applicability of the developed

sensors. As a result of these studies, the 4-AP-TOL-MIP(PP)/GCE sensor was stable for up to seven days, while the AA-TOL-MIP(TP)/GCE sensor was stable for only three days. The developed sensors showed good selectivity for TOL in the presence of interferents and also remarkable specificity compared to drugs of similar molecular structure (*i.e.* tolvaptan metabolite Tol-Ox, regorafenib, sorafenib, nilotinib, imatinib and dasatinib). In addition, the developed TOL sensors were successfully applied to tablets and commercial human serum samples. Based on the results obtained, these sensors can be used for TOL determination in quality control laboratories and potentially as wearable sensors to monitor drug concentrations in individuals.

Conflicts of interest

The authors have no conflicts of interest to declare.

Acknowledgements

F. B. thanks for the financial support from the Council of Higher Education (YOK) under the special 100/2000 scholarship program and the Scientific and Technological Research Council of Türkiye (TUBITAK) under the ARDEB/1004 Ph.D. Scholarship Programs. A. C. thanks the financial support from the Council of Higher Education (YOK) under the special 100/2000 scholarship program and the Scientific and Technological Research Council of Türkiye (TUBITAK) under the BIDEB/2211-A Ph.D. and ARDEB/1004 Ph.D. Scholarship Programs.

Notes and references

1 J. F. Dasta, J. R. Chiong, R. Christian, K. Friend, M. Lingohr-Smith, J. Lin and I. B. Cassidy, *http://dx.doi.org/10.1586/erp.12.30*, 2014, **12**, 399–410.

2 J. B. O'Connell and A. Alemayehu, *Postgrad. Med.*, 2012, **124**, 29–39.

3 M. Kadota, T. Ise, S. Yagi, T. Iwase, M. Akaike, R. Ueno, Y. Kawabata, T. Hara, K. Ogasawara, M. Band, S. Bando, T. Matsuura, K. Yamaguchi, H. Yamada, T. Soeki, T. Wakatsuki and M. Sata, *Int. Heart J.*, 2016, **57**, 461–465.

4 V. Ahluwalia, D. M. Heuman, G. Feldman, J. B. Wade, L. R. Thacker, E. Gavis, H. Gilles, A. Unser, M. B. White and J. S. Bajaj, *J. Hepatol.*, 2015, **62**, 75–82.

5 X. Ma, J. He, Y. Huang, Y. Xiao, Q. Wang and | Hui Li, *Wiley Online Libr.*, , DOI:10.1002/jmr.2598.

6 J. J. Beaudoin, J. Bezençon, Y. Cao, K. Mizuno, S. E. Roth, W. J. Brock and K. L. R. Brouwer, *Drug Metab. Dispos.*, 2019, **47**, 155–163.

7 K. S. Moola, B. S. R. Challa and C. K. Bannoth, *J. Pharm. Anal.*, 2015, **5**, 371–377.

8 M. Mazzarino, V. Buccilli, X. de la Torre, I. Fiacco, A. Palermo, D. Ughi and F. Botrè, *J. Pharm. Biomed. Anal.*, 2017, **145**, 555–568.

9 P. Guo, Q. Liang, J. Zheng, J. Chen, Y. Guan, L. Ding, F. Jiang, X. Chen, M. Huang, A. Chen and G. Zhong, *Bioanalysis*, 2020, **12**, 569–582.

10 V. R. Derangula, N. R. Pilli, B. R. Bhukya, C. R. Pulipati, V. Adireddy and V. Ponneri, *Biomed. Chromatogr.*, 2014, **28**, 332–340.

11 J. Jiang, L. Tian, Y. Huang, Y. Yan and Y. Li, *J. Chromatogr. B. Analyt. Technol. Biomed. Life Sci.*, 2016, **1027**, 158–164.

12 N. Khaleel and S. K. A. Rahaman, *Indian Drugs*, 2020, **57**, 62–68.

13 S. Rzeppa and L. N. Viet, *Drug Test. Anal.*, 2016, **8**, 1090–1094.

14 K. Hoshikawa, T. Naito, M. Saotome, Y. Maekawa and J. Kawakami, *Ann. Clin. Biochem.*, 2019, **56**, 387–396.

15 M. Furukawa, K. Miyata, C. Kawasome, Y. Himeda, K. Takeuchi, T. Koga, Y. Hirao and K. Umehara, *Arch. Pharm. Res.*, 2014, **37**, 1578–1587.

16 M. Furukawa, Y. Yamasaki, Y. Hirao and K. Umehara, *J. Chromatogr. B*, 2014, **965**, 112–118.

17 S. Akutsu, T. Naito, K. Hoshikawa, M. Saotome, Y. Maekawa and J. Kawakami, *J. Pharm. Biomed. Anal.*, 2020, **180**, 113061.

18 Q. Pei, B. Zhang, H. Tan, L. Liu, X. Peng, Z. Li, P. Huang, M. Luo, X. Zuo, C. Guo and G. Yang, *J. Chromatogr. B. Analyt. Technol. Biomed. Life Sci.*, 2013, **913**–**914**, 84–89.

19 U. J. Pandit, I. Khan, S. Wankar, K. K. Raj and S. N. Limaye, *Anal. Chem. Lett.*, 2015, **5**, 338–350.

20 G. Ozcelikay, A. Cetinkaya, E. B. Atici and S. A. Ozkan, *Anal. Methods*, 2023, **15**, 2309–2317.

21 Y. Dong, L. Yang and L. Zhang, *J. Agric. Food Chem.*, 2017, **65**, 727–736.

22 Y. Wang, X. Ma, Y. Peng, Y. Liu and H. Zhang, *J. Hazard. Mater.*, 2021, **416**, 126098.

23 X. Xie, X. Ma, L. Guo, Y. Fan, G. Zeng, M. Zhang and J. Li, *Chem. Eng. J.*, 2019, **357**, 56–65.

24 L. Karadurmus, M. E. Corman, L. Uzun and S. A. Ozkan, *Microchim. Acta*, , DOI:10.1007/s00604-022-05321-6.

25 L. Karadurmus, G. Ozcelikay, C. Armutcu and S. A. Ozkan, *Microchem. J.*, 2022, **181**, 107820.

